ACI MATERIALS JOURNAL TECHNICAL PAPER

Title no. 108-M36

Cracking and Healing of Engineered Cementitious Composites under Chloride Environment

by Mo Li and Victor C. Li

Engineered cementitious composite's (ECC) tensile ductility and microcracking behavior are essential for achieving structural durability (for example, corrosion resistance). This paper investigated ECC's durability in terms of maintaining its unique tensile characteristics under combined mechanical loading and aggressive chloride conditions. ECC specimens were preloaded to 0.5, 1.0, and 1.5% tensile strain levels; immersed in chloride solution for 30, 60, and 90 days; and reloaded until failure. This study revealed that the reloaded specimens retained multiple microcracking behavior and tensile strain capacity greater than 2.5%, while the average crack width increased from 50 μm to 100 μm. Self-healing in ECC under chloride exposure is evident in terms of recovery of initial material stiffness and tensile strain capacity. Subsequent studies at the microstructure scale explained the macroscopic composite behavior. These results indicated that under severe marine environmental conditions, ECC remains durable and provides reliable tensile ductility and crack-controlling capability to prevent the localized cracking failure often observed in concrete structures.

Keywords: corrosion; crack width; cracking; ductility; durability; engineered cementitious composites; reinforced concrete; self-healing.

INTRODUCTION

Concrete cracking is a result of the combined effects of mechanical loading conditions and environmental exposure.[1] Cracking can occur at different stages throughout the life of a concrete structure. The presence of cracks not only causes distress and loss of stiffness of structural members, but also dramatically lowers the resistance to penetration by aggressive agents (for example, chloride) that results in further deterioration.[2-4]

Among all possible forms of environmental exposure for concrete structures, concentrated chloride exposure (for example, in marine environments) is one of the most severe and aggressive.[5] Serious concrete deterioration has been reported, and the general cause was noted to be concrete cracking, which led to corrosion of embedded reinforcing steel and subsequent spalling of concrete cover.[6-9]

Maximum allowable crack widths are thereby required in various codes and specifications for the design of reinforced concrete structures exposed to aggressive chloride environments, as summarized in Fig. 1.[10-14] The allowable maximum crack width ranges from 150 to 300 μm (0.006 to 0.012 in.), with the most stringent requirements specified by JSCE and ACI 224R. According to ACI 224R, permissible crack width at the tensile face of reinforced concrete structures is 150 μm (0.006 in.) for exposure conditions of seawater, seawater spray, wetting, and drying; and 180 μm (0.007 in.) for deicing chemical exposure.

Such crack limits, however, are a challenge for traditional concrete materials due to their inherent brittleness and cracking tendency when subjected to mechanical loading conditions while also being attacked in aggressive environments. Despite extensive research, reliable crack width control using steel reinforcement in concrete structures remains difficult to realize in practice.[15-18] The new low-permeability concrete (also called high-performance concrete or high-strength concrete), made from partial substitution of portland cement with silica fume or fly ash, has recently been observed to have a more pronounced tendency to crack than conventional concrete.[19,20] With more finely-ground particles and lower water-cement ratio (*w/c*), high-strength concrete has higher early-age autogenous shrinkage, higher elastic modulus, and smaller creep deformation, and is therefore more susceptible to cracking.[21] This results in a faster, gravity-assisted flow of salt-laden water channels through the cracks, rather than a slow diffusion of chloride through uncracked concrete. Corrosion-inhibiting admixtures for concrete are not effective once cracks form.[22] Other corrosion control methods, such as epoxy-coated steel bars, need to be applied in conjunction with sound, crack-free concrete within structures, where the concrete is not constantly wet and other exposure conditions are not as severe.[23] These current limitations call for a new material-based approach to future concrete structures or repairs that intrinsically control crack width in order to resist chloride penetration and steel corrosion.

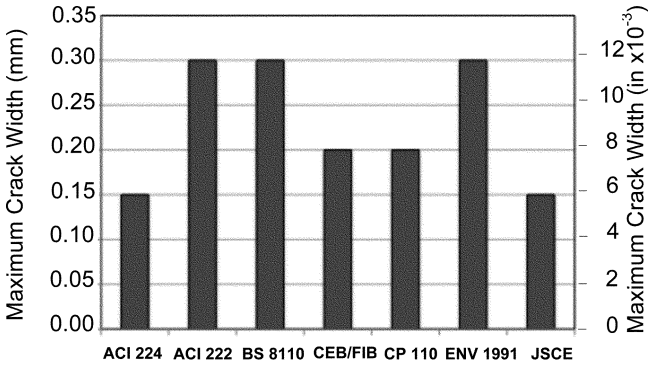

Fig. 1—Comparison of allowable crack widths under marine exposure.

Cracking control using strain-hardening ECC

Recent studies propose that the large tensile ductility of engineered cementitious composites (ECCs) achieved

ACI Materials Journal, V. 108, No. 3, May-June 2011.
MS No. M-2010-243 received August 10, 2010, and reviewed under Institute publication policies. Pertinent discussion including authors' closure, if any, will be published in the March-April 2012 *ACI Materials Journal* if the discussion is received by December 1, 2011.

ACI member **Mo Li** *is a Research Fellow in the Department of Civil and Environmental Engineering at the University of Michigan, Ann Arbor, MI. She received her BSE from Tongji University, China, and her MSE and PhD from the University of Michigan. Her research interests include the development, assessment, and implementation of new material technology for structural safety, durability, and sustainability.*

Victor C. Li, *FACI, is a Professor in the Department of Civil and Environmental Engineering at the University of Michigan. His research interests include the analysis, modeling, and design of ultra-ductile, green, and functional cementitious composites, their applications to innovative and sustainable infrastructure systems, and integration of materials and structural design.*

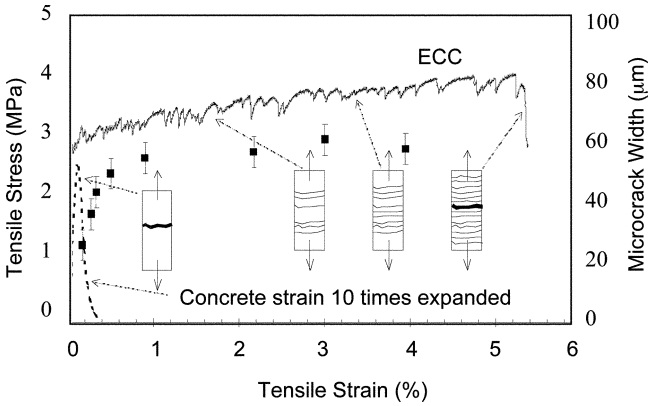

Fig. 2—Typical tensile stress-strain curve of ECC.

through multiple microcracking behavior, as well as its self-controlled crack width during the strain-hardening stage, are critical properties for achieving durability of reinforced concrete structures and repairs. ECC is a unique class of high-performance fiber-reinforced cementitious composites (HPFRCCs), micromechanically tailored to feature high intrinsic tensile ductility at moderate fiber content.[24,25] A typical uniaxial tensile stress-strain curve for ECC is shown in Fig. 2, along with averaged crack width development at different loading stages. With a fiber volume fraction no greater than 2%, ECC's tensile strain capacity is in the 2 to 5% range, which is around 200 to 500 times that of concrete and fiber-reinforced concrete (FRC).[26,27] The average crack width of ECC during the strain-hardening stage is below 60 μm (0.002 in.), and is independent of the applied deformation level and reinforcement ratio.[28] Such unique characteristics of ECC have been shown to suppress the most common mechanisms during the typical deterioration process in concrete structures[29] by preventing cracking and interfacial delamination caused by restrained volume change,[30] eliminating reflective cracking due to stress concentration under fatigue,[31] and enhancing resistance to chloride penetration and corrosion-induced cover spalling, even at large deformation levels.[32,33] ECC has been applied in new construction as well as in the repair of existing concrete structures.[34-37]

While ECC's large tensile ductility and self-controlled tight crack width are essential for ensuring structural durability, a question that could naturally be raised is whether ECC can still maintain these properties under combined mechanical loading and aggressive environmental (for example, chloride) exposure. This concern is critical because for many applications, especially concrete repair applications, ECC is expected to be in service during its strain-hardening stage.[31] At this stage, the imposed deformation due to restrained shrinkage, temperature effects, movement of underlying cracks, and structural loading would have activated various extents of multiple microcracking behavior. When exposed to an aggressive chloride environment, the chloride ions might penetrate through these cracks and reach the fibers and the fiber/matrix interface, leading to a loss of mechanical properties of ECC and its resistance to future superimposed deformation—for example, traffic loading, temperature change, or seismic loading.

The objective of the present study is to understand the long-term durability of ECC in both the cracked and uncracked state under a chloride environment. Specifically, the influence of different strain levels, combined with different chloride exposure durations, on the tensile ductility, cracking behavior, matrix, and fiber/matrix interface microparameters of ECC is investigated.

Evidence of self-healing of ECC microcracks

Self-healing of cracked concrete, commonly known as autogenous healing, is an often-studied phenomenon.[38,39] Self-healing is generally attributed to the hydration of previously unhydrated cementitious material, calcite formation, expansion of concrete in the crack flanks, crystallization, closing of cracks by solid matter in water, and closing of cracks by fragments of concrete from the cracks themselves.[40] It is believed that, under certain environmental conditions as well as in the presence of adequate concentrations of certain chemical species, the possibility and consistency of self-healing mechanisms greatly depend on crack width.[41] Previous studies have reported various ranges of maximum crack widths for self-healing to occur in concrete under various environmental exposure conditions: 5 to 10 μm,[42] 53 μm,[43] 100 μm,[44] 150 μm,[32] 200 μm,[45] 205 μm,[46] and 300 μm.[47] These results, despite their wide range, imply that a tighter crack width is favorable for self-healing to occur within the crack. A tight crack width, however, is difficult to achieve consistently in normal concrete; reliable self-healing has not been observed in most concrete structures.

The self-healing phenomenon in ECC at the composite scale under various exposure regimes, including water/air cycle, water/hot air cycle, 90%RH/air cycle, water submersion, and air, have been reported previously.[38,39,48] The chloride exposure regime had not been investigated until a recent study observed recovery of chloride transport properties in preloaded ECC beam specimens, indicating autogenous self-healing phenomenon.[32] The possibility of autogenous self-healing in preloaded ECC specimens exposed to a chloride environment, in terms of recovery of mechanical properties, was not previously understood, either at the composite or microstructure level.

To investigate this phenomenon in this study, ECC specimens were preloaded under uniaxial tension to strain levels of 0.5%, 1.0%, and 1.5% to simulate in-service loading conditions (for example, vehicle load, prestressing load, restrained shrinkage, and thermal load). After applying and removing the load, specimens exhibiting different extents of microcracking were exposed to a 3% chloride concentration solution for 1, 2, or 3 months and subsequently reloaded until failure to measure residual tensile properties. The effect of cracking and autogenous healing in ECC under combined mechanical loading and chloride exposure was assessed by measuring the retained stiffness, ultimate tensile strength, tensile strain capacity, and crack width. The influence of chloride exposure on ECC matrix and fiber/matrix interfacial properties was also studied.

RESEARCH SIGNIFICANCE

Worldwide, the premature deterioration of concrete structures due to corrosion of embedded steel has caused great economic, environmental, and social concern. Current concrete materials, especially high-strength concrete, are susceptible to cracking due to their brittle nature, which greatly compromises resistance to chloride penetration and cover spalling. Such limitations call for new, nonbrittle concrete materials, such as ECC, which intrinsically controls cracking and exhibits large tensile ductility to suppress cover spalling. This research proves that ECC is durable in both its microcracked and uncracked states under aggressive chloride environment, thus providing its unique cracking control capability and ductility to combat corrosion-induced deterioration in concrete structures.

EXPERIMENTAL INVESTIGATION

Materials and mixture proportions

The mixture proportions of ECC (M45, the most commonly studied version) are summarized in Table 1. Similar to typical FRCs, ECC M45 consists of Type I portland cement, sand, Class F fly ash, water, fibers, and a high-range water-reducing admixture. Unlike typical FRCs, however, the component characteristics and proportions within ECC were carefully determined through micromechanical design tools, so that the three phases (fibers, cementitious matrix, and fiber/matrix interface) work synergistically to achieve composite strain-hardening response.[49] To minimize the mortar matrix crack tip fracture energy, no coarse aggregates were used. Instead, fine silica sand with average and maximum grain sizes of 110 and 200 μm (0.004 and 0.008 in.), respectively, was adopted. The polyvinyl alcohol (PVA) fibers were manufactured with an aspect ratio, tensile strength, elastic modulus, and maximum elongation to meet the micromechanical design criteria for strain-hardening performance. The PVA fiber surface was coated with a small amount (1.2% by weight) of a proprietary hydrophobic agent to control the fiber/matrix interfacial properties for strain-hardening behavior.[50] The mechanical and geometrical properties of the PVA fibers used in this study are shown in Table 2.

Testing of composite properties

The ECC mixture was prepared in a Hobart mixer according to the following procedure: the cement, fly ash and sand were first mixed for 1 minute. Water and the high-range water-reducing admixture were then slowly added and mixed for two additional minutes at which point the cementitious material attained a homogeneous state. Finally, the fibers were added and mixed for 2 to 3 minutes until maximum uniformity of fiber dispersion was achieved. This mixture was cast into 152.4 x 76.2 x 12.7 mm (9 x 3 x 0.5 in.) tensile specimens. The specimens were covered with plastic sheets and demolded after 24 hours. They were first cured in plastic bags at 95 ± 5% relative humidity (RH), 20 ± 1°C (66 to 70°F) for six additional days and then left to cure in laboratory air under controlled humidity (45 ± 5% RH) and temperature (20 ± 1°C [66 to 70°F]) conditions until the age of 28 days for testing.

The magnitude of initial and retained mechanical properties was measured under uniaxial tensile loading. The direct uniaxial tensile test is considered the most convincing method for evaluating material strain-hardening behavior because some quasi-brittle FRC can also show apparent hardening behavior under flexural loading—a phenomenon known as "deflection hardening."[51] The tensile specimen dimensions and testing setup are shown in Fig. 3.

First, different levels of preloading under tension were imposed on the composite specimens to the strain of 0, 0.5, 1.0, and 1.5%, followed by unloading before exposure to 3% NaCl solution. Prior to composite tensile testing, four aluminum plates were glued to the four edges of the specimen to facilitate gripping. Tests were conducted on a servo-hydraulic testing system with 25 kN (5.62 kip) capacity, under a displacement control with rate of 0.005 mm/s (1.97×10^{-4} in./s). Two external linear variable differential transformers (LVDTs) were attached to the specimen surface, with a gauge length of 101.6 mm (4 in.), to measure the displacement.

Table 1—Mixture proportions and properties of ECC (M45)

Properties	ECC (M45)
FA/C	1.2
W/(C+FA)	0.27
Water (W), kg/m^3 (lb/yd^3)	331 (558)
Cement (C), kg/m^3 (lb/yd^3)	570 (961)
Fly ash (FA), kg/m^3 (lb/yd^3)	684 (1153)
Sand (S), kg/m^3 (lb/yd^3)	455 (767)
Fiber (PVA), kg/m^3 (lb/yd^3)	26 (44)
Superplasticizer (SP), kg/m^3 (lb/yd^3)	5.1 (8.6)
7-day compressive strength, MPa (ksi)	37.8 (5.5)
28-day compressive strength, MPa (ksi)	53.3 (7.7)
7-day tensile strain capacity, %	3.90
28-day tensile strain capacity, %	3.10

Table 2—Properties of PVA fiber

Nominal strength, MPa (ksi)	Apparent strength, MPa (ksi)	Diameter, μm (in.)	Length, mm (in.)	Young's modulus, GPa (ksi)	Elongation, %
1620 (235)	1092 (158)	39 (0.002)	8 (0.3)	42.8 (6200)	6.0

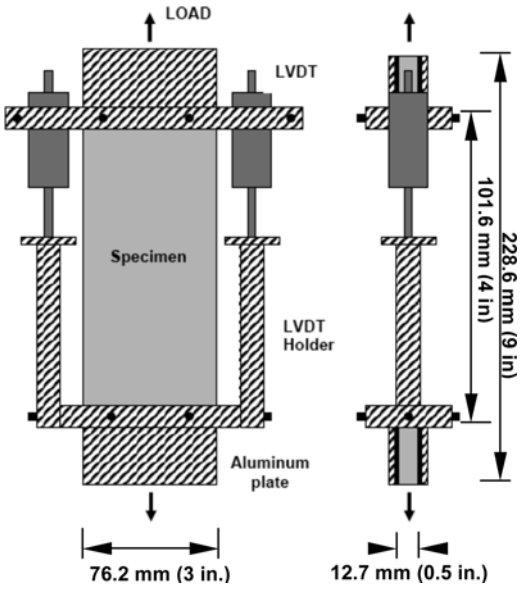

Fig. 3—Uniaxial tensile test setup and specimen dimensions.

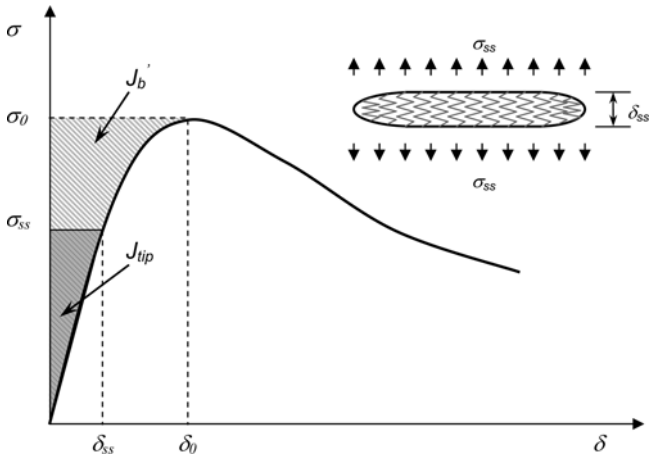

Fig. 4—Typical fiber bridging stress versus cracking opening $\sigma(\delta)$ curve for tensile strain hardening composite. Hatched area represents complimentary energy J_b'. Shaded area represents crack tip toughness J_{tip}.

Specimens were preloaded at the age of 28 days, measured as the time between the end of casting and the start of testing.

The preloaded ECC specimens, together with specimens that were not subjected to preloading (preloading strain = 0), were then immersed in a 3% NaCl solution under controlled room temperature 20 ± 1°C (66 to 70°F) for 30, 60, or 90 days, respectively. In addition, control specimens that were not preloaded or immersed in the solution were stored in the air at room temperature 20 ± 1°C (66 to 70°F) and 45 ± 5% RH for 30, 60, or 90 days. Subsequently, the preloaded specimens were reloaded in direct tension. Their stress-strain curves were measured and compared to those of the non-preloaded specimens (cured in air or chloride solution) that were also subjected to direct tension at the same ages. Six specimens were tested for each case.

Measurement of micromechanical parameters

To understand the potential effects of chloride exposure on ECC matrix and fiber/matrix interfacial properties at the micromechanical scale, a matrix fracture toughness test and a single-fiber pullout test were conducted.

The tensile strain-hardening behavior of ECC is realized by the synergistic interaction between the fibers, matrix, and fiber/matrix interface based on micromechanics theory. As a fiber-reinforced brittle mortar matrix composite, ECC's pseudo strain-hardening behavior is achieved through sequential formation of matrix multiple cracking. The fundamental requirement for matrix multiple cracking is that steady-state flat crack propagation prevails under tension.[52,53] To ensure steady-state cracking, the crack tip toughness J_{tip} must be less than the complementary energy J_b' calculated from the fiber bridging stress σ versus crack opening δ relation, as illustrated in Fig. 4 and shown in Eq. (1) and (2).

$$J_{tip} \le \sigma_0\delta_0 - \int_0^{\delta_0}\sigma(\delta)d\delta \equiv J_b' \quad (1)$$

$$J_{tip} = \frac{K_m^2}{E_m} \quad (2)$$

where σ_0 is the maximum bridging stress corresponding to the opening δ_0; K_m is the matrix fracture toughness; and E_m is the matrix Young's modulus. Equation (1) employs the concept of energy balance during flat crack extension between external work ($\sigma_0\delta_0$), crack flank energy absorption through fiber/matrix interface debonding and sliding ($\int_0^{\delta_0}\sigma(\delta)d\delta$), and crack tip energy absorption through matrix breakdown (J_{tip}). This energy-based criterion determines whether the crack propagation mode is steady-state flat cracking or Griffith cracking.[54]

Apart from the energy criterion, another condition for pseudo strain hardening is that the matrix tensile cracking strength σ_c must not exceed the maximum fiber bridging strength σ_0.

$$\sigma_c < \sigma_0 \quad (3)$$

where σ_c is determined by the matrix fracture toughness K_m and pre-existing internal flaw size a_0. While the energy criterion (Eq. (1)) governs the crack propagation mode, the strength-based criterion (Eq. (3)) controls the initiation of cracks. Satisfaction of both equations is necessary to achieve ECC strain-hardening behavior; otherwise, the composite behaves as a normal fiber-reinforced concrete (FRC) and tension-softening behavior results.

High tensile strain capacity requires a high J_b'/J_{tip} ratio, also called the pseudo strain-hardening (PSH) index. J_{tip} is determined by matrix properties, whereas J_b' is governed by fiber and interface properties.

To measure J_{tip}, matrix toughness tests were conducted on the ECC matrix (without fibers) specimens before and after exposure to 3% NaCl solution for 30, 60, and 90 days, respectively. This test was based on ASTM E399,[55] which allows one to use different geometry specimens, such as bending specimens and compact tension specimens, to measure the K_m value. The fresh mixture was cast into notched beam specimens measuring 305 mm (12 in.) in length, 76 mm (3 in.) in height, and 38 mm (1.5 in.) in thickness. The specimens were then demolded at 24 hours, first cured in plastic bags at 95 ± 5% RH, 20 ± 1°C (66 to 70°F) for six additional days, and then left to cure in laboratory air at 45 ± 5% RH and 20 ± 1°C (66 to 70°F) until the age of 28 days. The specimens were then stored in 3% NaCl solution for 0, 30, 60, and 90 days.

The matrix fracture toughness K_m was measured by the three-point bending test, as shown in Fig. 5. The support span was 254 mm (10 in.) and the notch depth-to-height ratio was 0.4. Six specimens were tested for each scenario. J_{tip} was calculated from the measured K_m through Eq. (2).

To calculate J_b', single-fiber pullout tests were conducted to measure three fiber/matrix interfacial parameters: chemical bond strength G_d, frictional bond strength τ_0, and slip hardening coefficient β. As shown in Fig. 6, single-fiber pullout tests were conducted on small-scale prismatic specimens with dimensions of 10 x 10 x 0.5 mm (0.4 x 0.4 x 0.02 in.). A single fiber was aligned and embedded into the center of an ECC mortar prism with an embedment length of 0.5 mm (0.02 in.). The specimens were demolded at 24 hours, first cured in plastic bags at 95 ± 5% RH, 20 ± 1°C (66 to 70°F) for six additional days, and then left to cure in laboratory air

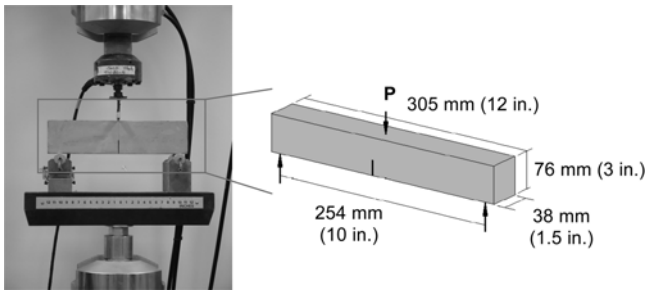

Fig. 5—Matrix fracture toughness test setup and specimen dimensions.

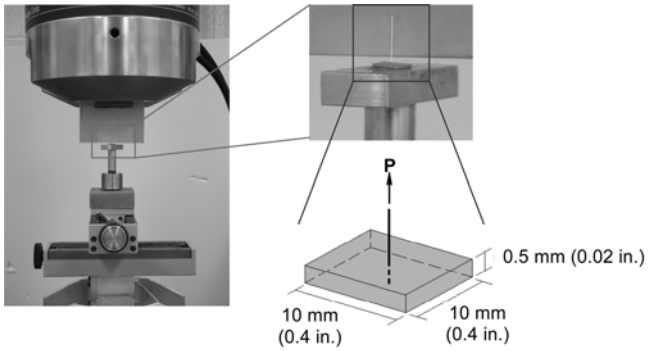

Fig. 6—Single-fiber pullout test setup and specimen dimensions.

under 45 ± 5% RH and 20 ± 1°C (66 to 70°F) until the age of 28 days. The specimens were then stored in 3% NaCl solution for 0, 30, 60, and 90 days. Ten specimens were tested for each scenario. The load-versus-displacement curve was obtained through quasi-static testing and used to determine G_d, τ_0, and β. These interfacial parameters, along with fiber volume fraction, length, and diameter, were then used to calculate the fiber bridging law $\sigma(\delta)$ based on the theoretical model described in Li and Leung.[53] The resulting complementary energy J_b', determined from the $\sigma(\delta)$ curve, combined with the matrix fracture toughness J_{tip} obtained from the K_m measurement, were used to calculate the PSH (J_b'/J_{tip}) index and to evaluate composite material behavior (that is, strain-hardening or tension-softening).

EXPERIMENTAL RESULTS AND DISCUSSION

Table 3 summarizes the tensile strain capacity, ultimate tensile strength, and average crack width of ECC with various preloaded strain levels and chloride exposure durations. Typical tensile stress-strain curves obtained for specimens before and after exposure to the chloride solution are shown in Fig. 7. The ultimate tensile strength and tensile strain capacity are defined as the peak stress and corresponding strain values on the tensile stress-strain curve, respectively. The first-cracking strength is determined as the stress value when the first microcrack occurs in the specimen, and corresponds to the first stress drop on the tensile stress-strain curve. For the same-age uncracked specimens that were not preloaded, those exposed to chloride solution exhibited ultimate tensile strength 5 to 10% lower than those cured in air (Table 3). The first-cracking strength was also reduced by 20 to 33%. However, the tensile strain capacity did not appear to be affected after 30, 60, and 90 days of chloride exposure. Multiple microcracking behavior was retained

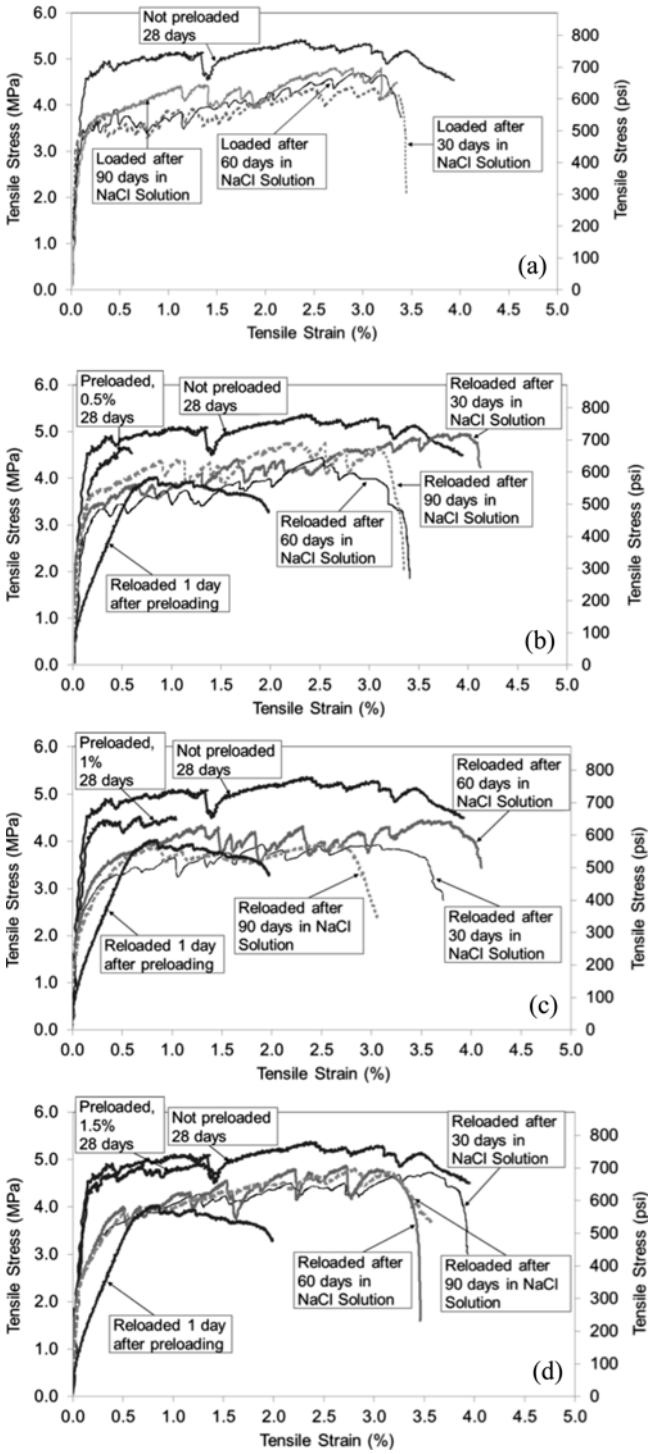

Fig. 7—Tensile stress-strain curves of ECC specimens before and after exposure to 3% NaCl solution: (a) not preloaded; (b) preloaded to 0.5% tensile strain; (c) preloaded to 1.0% tensile strain; and (d) preloaded to 1.5% tensile strain.

after 30, 60, and 90 days of chloride exposure, while the average crack width increased from 50 μm (air curing) to 100 μm (chloride exposure). Chloride exposure similarly affected the preloaded specimens in terms of reduction in first-cracking strength and ultimate tensile strength (by 7 to 13%), increase in crack width, and maintained tensile ductility and multiple microcracking behavior. However, applied tensile strain up to 1.5% did not exacerbate deterioration.

Table 3—Tensile properties of ECC under different combinations of preloading levels and air/chloride exposure durations

Environmental exposure condition	Preloaded strain, %	Tensile strain capacity, %	Ultimate tensile strength, MPa (psi)	Average crack width, μm (× 10^{-3} in.)
28 days air + 30 days air or NaCl	0.0 (air curing)	2.86 ± 0.58	4.81 ± 0.64 (698 ± 93)	50 (2.0)
	0.0 (3% NaCl)	2.79 ± 0.54	4.34 ± 0.62 (629 ± 90)	100 (3.9)
	0.5 (3% NaCl)	3.85 ± 0.61	4.59 ± 0.29 (666 ± 42)	100 (3.9)
	1.0 (3% NaCl)	2.66 ± 0.66	3.85 ± 0.59 (558 ± 86)	100 (3.9)
	1.5 (3% NaCl)	2.48 ± 0.94	4.24 ± 0.73 (615 ± 106)	100 (3.9)
28 days air + 60 days air or NaCl	0.0 (air curing)	2.51 ± 0.19	4.75 ± 0.45 (689 ± 65)	40 (1.6)
	0.0 (3% NaCl)	2.37 ± 0.50	4.25 ± 0.47 (616 ± 68)	100 (3.9)
	0.5 (3% NaCl)	3.16 ± 0.26	4.05 ± 0.47 (587 ± 68)	100 (3.9)
	1.0 (3% NaCl)	3.28 ± 0.42	4.18 ± 0.22 (606 ± 32)	100 (3.9)
	1.5 (3% NaCl)	2.97 ± 0.69	4.07 ± 0.47 (590 ± 68)	80 (3.1)
28 days air + 90 days air or NaCl	0.0 (air curing)	3.02 ± 0.60	4.64 ± 0.32 (673 ± 46)	40 (1.6)
	0.0 (3% NaCl)	3.27 ± 0.76	4.41 + 0.45 (640 ± 65)	100 (3.9)
	0.5 (3% NaCl)	3.22 ± 0.39	4.70 ± 0.35 (682 ± 51)	100 (3.9)
	1.0 (3% NaCl)	2.61 ± 0.12	4.12 ± 0.17 (598 ± 25)	80 (1.6)
	1.5 (3% NaCl)	2.96 ± 0.87	4.12 ± 0.25 (598 ± 36)	90 (3.5)

Figure 7 also shows the tensile properties of ECC specimens preloaded to 0.5, 1.0, and 1.5% strain levels, then unloaded and reloaded 1 day after precracking. These specimens did not undergo the crack healing as compared to those exposed to chloride solution for 30, 60, and 90 days. Therefore, they exhibited a remarkable loss in initial stiffness, which was defined by the slope of the initial linear segment on the stress-strain curve. This was due to the low load resistance provided by re-opening the existing microcracks before bridging fibers were re-engaged. Once fiber bridging was re-engaged, however, the load capacity resumed and further tensile straining of the intact material took place.

In contrast, a significant recovery of the initial material stiffness was found in the preloaded ECC specimens after they were exposed to chloride solution for 30, 60, and 90 days and then reloaded. This suggested that healing of the microcracks took place in the ECC specimens after exposure to chloride solution, and led to the stiffness recovery as reloading stressed the self-healing products within the microcracks. Self-healing can be attributed primarily to the availability of unhydrated cement due to the low water-to-binder ratio within the ECC mixture as well as the pozzolanic reaction of the fly ash. After precracking, these cementitious and pozzolanic particles on crack surfaces were readily exposed to the chloride solution and initiated further hydration and pozzolanic processes. The presence of chloride ions might accelerate the hydration process. The newly formed products not only physically sealed the microcracks and recovered ECC transport properties, but also recovered the fiber-bridging mechanism by reforming the fiber/matrix interfacial bond at the microcracks, and thus restored the composite tensile properties.

Compared to the same-age control specimens cured in air, the preloaded specimens immersed in chloride solution showed a 7 to 13% reduction in ultimate tensile strength. This should be attributed to the effects of calcium hydroxide leaching on the fiber/matrix interfacial bond that lowered fiber-bridging capacity. Water not saturated with calcium hydroxide (high-calcium hydrated lime) may affect test results due to the leaching of lime from the test specimens.[56] The presence of chloride ions tends to increase the leaching of calcium and porosity of the cementitious matrix.[57,58]

The tensile strain capacity reported for these specimens does not include the residual strain following the precracking load. By neglecting this residual strain, the large variability in material relaxation during unloading was avoided, and a conservative estimate of ultimate strain capacity of the material was determined. The average tensile strain capacity of uncracked and precracked ECC specimens exposed to chloride solution ranged between 2.48% and 3.85%. These values were on the same level with or higher than those of air-cured specimens, which ranged from 2.51% to 3.02%.

The influence of chloride exposure on non-preloaded ECC composite tensile properties can be explained by its effect on the microstructure of ECC. Kabele et al.[59] studied the exposure scenario of 10 cycles of 5-day immersion in a saturated solution of NaCl at 20°C (68°F) and 2-day drying in oven at 50°C (122°F), and found negligible decrease in ECC matrix toughness, a significant reduction in interfacial chemical bond G_d, and an increase in interfacial frictional bond τ_0. From the measured micromechanical parameters in this study, a 17 to 20% reduction in matrix fracture toughness K_m, or crack tip energy J_{tip} (Fig. 8(a)), was found after the specimens were exposed to chloride solution for 30, 60, and 90 days. The matrix toughness reduction, highly possibly due to the leaching of calcium hydroxide in the cementitious matrix to the chloride solution and the corresponding increase in matrix porosity, explained the reduction in ECC's first-cracking strength at the composite scale. In Fig. 8(b) and (c), despite the large error bar typical of the single-fiber pullout test, it was observed that both the interfacial chemical bond G_d and frictional bond τ_0 tended to decrease after 30, 60, and 90 days of exposure to chloride solution. The reduction in the fiber/matrix interfacial bonds can be attributed to the leaching of calcium hydroxide and increased porosity at the fiber/matrix interfacial transition zone, which was accelerated by chloride ions, and the presence of chloride ions and moisture at the interface that potentially harmed the interfacial bonds. The reduction in interfacial bonds explained the increase in crack width in ECC composites from less than 50 μm before chloride exposure, to approximately 100 μm after 30, 60, or 90 days of chloride exposure. Furthermore, the reduction in interfacial bonds also led to a decrease in fiber-

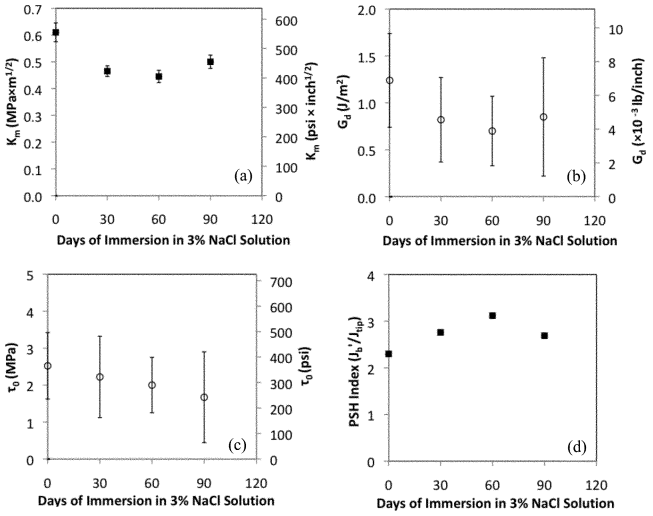

Fig. 8—Influence of 3% NaCl solution exposure time on ECC microparameters: (a) matrix fracture toughness K_m*; (b) fiber/matrix interfacial chemical bond* G_d*; (c) fiber/matrix interfacial frictional bond* τ_0*; and (d) PSH index.*

bridging capacity σ_0 (Fig. 4), resulting in the 5 to 10% reduction in ECC composite ultimate tensile strength.

The calculated PSH index, J_b'/J_{tip}, is shown in Fig. 8(d). Interestingly, it was found that the PSH index increased from 2.3 (before chloride exposure) to 2.8 (30-day chloride exposure), 3.1 (60-day chloride exposure), and 2.7 (90-day chloride exposure). This suggested that, after different durations of severe chloride exposure, the PSH index did not decline but instead increased. This clarified the underlying micromechanical mechanism of the retention of tensile strain capacity of ECC composites after 30, 60, and 90 days of chloride exposure. Such a mechanism does not exist in traditional concrete materials because the leaching of calcium hydroxide only impairs concrete mechanical properties (for example, tensile cracking strength), thereby promoting concrete deterioration.[57,58] However, the reduction of PSH from 3.1 at 60-day exposure to 2.7 at 90-day exposure suggests that the time duration of exposure should be further extended in future studies until steady state is reached.

CONCLUSIONS

From this experimental study, it is preliminarily concluded that ECC remains durable under combined mechanical loading and exposure to a high chloride concentration environment. The ECC investigated maintained its unique tensile ductility and multiple microcracking behavior under combined mechanical loading conditions (0.5%, 1.0%, 1.5% tensile straining and reloading to failure) and aggressive chloride exposure (30-, 60-, and 90-day immersion in 3% NaCl solution). It suggested that even under severe marine environment conditions, ECC retains a robust tensile ductility that prevents the common failure mechanisms in concrete structures such as cracking due to restrained volume change, stress concentration, or fatigue, despite the observed reduction in first-cracking strength and ultimate tensile strength. Additionally, its self-controlled microcrack width during the strain-hardening stage can provide reliable resistance to chloride penetration, even under large applied strain (or loading) levels while simultaneously subjected to aggressive chloride exposure. Although the average crack width of ECC does increase from 50 μm to 100 μm, it is still below the maximum crack width limit allowed by various design codes for marine environments.

This study reveals the ability of ECC to self-heal crack damage in a high chloride concentration environment. Similar to self-healing behavior in a water environment, nearly complete recovery of material stiffness and tensile strain capacity due to self-healing was found in ECC that has been loaded up to 1.5% tensile strain and immersed in 3% NaCl solution for 30 days or more.

From the micromechanics experimental study, it is concluded that the general descending trends of ECC matrix toughness as well as its interface frictional and chemical bonds in the presence of concentrated chloride solution are responsible for the reduced ECC first-cracking strength and the modification of the PVA fiber bridging behavior. A reduction in chemical bonding of the PVA fiber to the mortar matrix results in lower ECC ultimate tensile strength and an increase in ECC microcrack width, as experimentally observed in this study. The presence of chloride ions was believed to promote the leaching of calcium hydroxide and consequently increased porosity in the cementitious matrix and the fiber/matrix interfacial transition zone. The changes in both matrix toughness and interfacial properties led to a slight increase in the PSH index J_b'/J_{tip}, which was favorable for multiple microcracking that retained the tensile strain capacity in ECC.

The conclusions drawn from this study are based on 3% concentration chloride exposure with duration up to 90 days. In the future, it is advisable to perform exposure experiments in field conditions (for example, a marine environment) for years to assess the longer-term durability and self-healing robustness of ECC.

ACKNOWLEDGMENTS

The authors would like to thank the Michigan DOT and the U.S. National Science Foundation MUSES Grant (CMS-0223971) and Civil Infrastructure Grant (CMMI 0700219) for partial funding of this research.

REFERENCES

1. ACI Committee 224, "Control of Cracking in Concrete Structures (ACI 224R-01)," American Concrete Institute, Farmington Hills, MI, 2001, 45 pp.

2. McKeel, W. T., "Evaluation of Deck Durability on Continuous Beam Highway Bridges," *Report* No. VHTRC 85-R32, Virginia Highway and Transportation Research Council, Charlottesville, VA, 1985.

3. Perfetti, G. R.; Johnson, D. W.; and Bingham, W. L., "Incidence Assessment of Transverse Cracking in Concrete Bridge Decks: Structural Considerations," *Report* No. FHWA/NC/85-002, V. 2, Federal Highway Administration, Washington, DC, 1985.

4. Oh, B. H.; Cha, S. W.; Jang, B. S.; and Jang, S. Y., "Development of High-Performance Concrete Having High Resistance to Chloride Penetration," *Nuclear Engineering and Design* (Switzerland), V. 212, No. 1-3, 2002, pp. 221-231.

5. Tsinker, G. P., *Marine Structures Engineering: Specialized Applications*, 1995, 548 pp.

6. Mehta, P. K., and Gerwick, B. C., "Cracking-Corrosion Interaction in Concrete Exposed to Marine Environment," *Concrete International*, V. 4, No. 10, Oct. 1982, pp. 45-51.

7. Gilbride, P.; Morgan, D. R.; and Bremner, T. W., "Deterioration and Rehabilitation of Berth Faces in Tidal Zones at the Port of Saint John," *Shotcrete*, Fall 2002, pp. 32-38.

8. Mehta, P. K., "Durability of Concrete Exposed to Marine Environment—A Fresh Look," *Concrete in Marine Environment*, SP-109, American Concrete Institute, Farmington Hills, MI, 1988, pp. 1-30.

9. Liu, P. C., "Damage to Concrete Structures in a Marine Environment," *Materials and Structures*, V. 24, 1991, pp. 302-307.

10. British Standards Institution, "BS 8110: Part 1," BSI, London, 1997.

11. CEB-FIP Model Code 1990, *CEB Information Report* No. 213/214, Comite Euro-International Du Beton, Lausanne, May 1993.

12. "Code of Practice for the Structural Use of Concrete—Part 1. Design, Materials and Workmanship," *British Standards Institution Publication CP 110*, London, UK, Nov. 1972 (amended May 1977).

13. "Standard Specification for Design and Construction of Concrete Structures—1986, Part 1 (Design)," Japan Society of Civil Engineers, SP-1, Tokyo, Japan, 1986.

14. ACI Committee 222, "Corrosion of Metals in Concrete (ACI 222R-89)," American Concrete Institute, Farmington Hills, MI, 1989, 30 pp.

15. Markeset, G.; Rostam, S.; and Klinghoffer, O., "Guild for the Use of Stainless Steel Reinforcement in Concrete Structures," *Project Report 405*, Nordic Innovation Center Project – 04118: Corrosion Resistant Steel Reinforcement in Concrete Structures (NonCor), 2006, p. 59.

16. Vaysburd, A. M.; Emmons, P. H.; Mailvaganam, N. P.; McDonald, J. E.; and Bissonnette, B., "Concrete Repair Technology—A Revised Approach is Needed," *Concrete International*, V. 26, No. 1, Jan. 2004, pp. 58-65.

17. Cusson, D., and Mailvaganam, N., "Durability of Repair Materials," *Concrete International*, V. 18, No. 3, Mar. 1996, pp. 34-38.

18. Grzybowski, M., and Shah, S. P., "Shrinkage Cracking of Fiber Reinforced Concrete," *ACI Materials Journal*, V. 87, No. 2, Mar.-Apr. 1990, pp. 138-148.

19. Mehta, P. K., "Durability—Critical Issues for the Future," *Concrete International*, V. 19, No. 6, June 1997, pp. 27-33.

20. Xi, Y.; Shing, B.; Abu-Hejleh, N.; Asiz, A.; Suwito, A.; Xie, Z.; and Ababneh, A., "Assessment of the Cracking Problem in Newly Constructed Bridge Decks in Colorado," CDOT-DTD-R-2003-3, Colorado Department of Transportation Research Branch, Denver, CO, Mar. 2003.

21. Shah, S. P.; Wang, K.; and Weiss, W. J., "Is High Strength Concrete Durable?" *Concrete Technology for a Sustainable Development in the 21st Century*, O. E. Gjørv and K. Sakai, eds., 2000, pp. 102-114.

22. Kondratova, I., and Bremner, T. W., "Field and Laboratory Performance of Epoxy-Coated Reinforcement in Cracked and Uncracked Concrete," Presented at the 77th Annual Meeting of the Transportation Research Board, Washington, DC, 1998.

23. Whiting, D.; Nagi, M.; and Broomfield, J. P., "Evaluation of Sacrificial Anode for Cathodic Protection of Reinforced Concrete Bridge Decks," *Report* No. FHWA-RD-95-041, Federal Highway Administration, Washington, DC, May 1995.

24. Li, V. C., "Reflections on the Research and Development of Engineered Cementitious Composites (ECC)," *Proceedings of the JCI International Workshop on Ductile Fiber Reinforced Cementitious Composites (DFRCC)—Application and Evaluation (DRFCC-2002)*, Takayama, Japan, Oct. 2002, pp. 1-21.

25. Li, V. C., "Integrated Structures and Materials Design," *Journal of Materials and Structures*, RILEM, V. 40, No. 4, 2007, pp. 387-396.

26. Li, V. C., "Engineered Cementitious Composites—Tailored Composites through Micromechanical Modeling," *Fiber Reinforced Concrete: Present and the Future*, N. Banthia, A. A. Bentur, and A. Mufti, eds., Canadian Society for Civil Engineering, Montreal, QC, Canada, 1998, pp. 64-97.

27. Li, V. C.; Wu, C.; Wang, S.; Ogawa, A.; and Saito, T., "Interface Tailoring for Strain-Hardening Polyvinyl Alcohol-Engineered Cementitious Composites (PVA-ECC)," *ACI Materials Journal*, V. 99, No. 5, Sept.-Oct. 2002, pp. 463-472.

28. Maalej, M.; Hashida, T.; and Li, V. C., "Effect of Fiber Volume Fraction on the Off-Crack Plane Energy in Strain-Hardening Engineered Cementitious Composites," *Journal of the American Ceramics Society*, V. 78, No. 12, 1995, pp. 3369-3375.

29. Li, V. C., and Li, M., "Durability Performance of Ductile Concrete Structures," *Proceedings of the 8th International Conference on Creep, Shrinkage and Durability of Concrete and Concrete Structures*, Tanabe et al., eds., Ise-Shima, Japan, Sept.-Oct. 2008, pp. 761-768.

30. Li, M., and Li, V. C., "Influence of Material Ductility on the Performance of Concrete Repair," *ACI Materials Journal*, V. 106, No. 5, Sept.-Oct. 2009, pp. 419-428.

31. Li, M., "Multi-Scale Design for Durable Repair of Concrete Structures," PhD dissertation, University of Michigan, Ann Arbor, MI, 2009, 425 pp.

32. Sahmaran, M.; Li, M.; and Li, V. C., "Transport Properties of Engineered Cementitious Composites Under Chloride Exposure," *ACI Materials Journal*, V. 104, No. 6, Nov.-Dec. 2007, pp. 604-611.

33. Sahmaran, M.; Li, V. C.; and Andrade, C., "Corrosion Resistance Performance of Steel-Reinforced Engineered Cementitious Composite Beams," *ACI Materials Journal*, V. 105, No. 3, May-June 2008, pp. 243-250.

34. Li, V. C.; Lepech, M.; and Li, M., "Field Demonstration of Durable Link Slabs for Jointless Bridge Decks Based on Strain-Hardening Cementitious Composites," *Michigan DOT Report RC-1471*, Dec. 2005.

35. Li, V. C.; Li, M.; and Lepech, M., "High Performance Material for Rapid Durable Repair of Bridges and Structures," *Michigan DOT Report RC-1484*, Dec. 2006.

36. Kunieda, M., and Rokugo, K., "Recent Progress on HPFRCC in Japan," *Journal of Advanced Concrete Technology*, V. 4, No. 1, 2006, pp. 19-33.

37. Li, V. C.; Fischer, G.; and Lepech, M., "Shotcreting with ECC," Proceedings, W. Kusterle, ed., Spritzbeton-Tagung, Austria, 2009. (CD-ROM)

38. Yang, E. H., "Designing Added Functions in Engineered Cementitious Composites," PhD dissertation, University of Michigan, Ann Arbor, MI, 2008.

39. Yang, Y. Z.; Lepech, M. D.; and Li, V. C., "Self-Healing of Engineered Cementitious Composites under Cyclic Wetting and Drying," *Proceedings of the International Workshop on Durability of Reinforced Concrete under Combined Mechanical and Climatic Loads (CMCL)*, Qingdao, China, Oct. 2005, pp. 231-242.

40. Ramm, W., and Biscoping, M., "Autogenous Healing and Reinforcement Corrosion of Water-Penetrated Separation Cracks in Reinforced Concrete," *Nuclear Engineering and Design*, V. 179, 1998, pp. 191-200.

41. Li, V. C., and Yang, E. H., "Self Healing in Concrete Materials," *Self Healing Materials: An Alternative Approach to 20 Centuries of Materials*, 2007, pp. 160-194.

42. Jacobsen, S.; Marchand, J.; and Homain, H., "SEM Observations of the Microstructure of Frost Deteriorated and Self-Healed Concrete," *Journal of Cement and Concrete Research*, V. 25, 1995, pp. 1781-1790.

43. Ismail, M.; Toumi, A.; Francois, R.; and Gagne, R., "Effect of Crack Opening on Local Diffusion of Chloride Inert Materials," *Cement and Concrete Research*, V. 34, 2004, pp. 711-716.

44. Reinhardt, H., and Joos, M., "Permeability and Self-Healing of Cracked Concrete as a Function of Temperature and Crack Width," *Journal of Cement and Concrete Research*, V. 33, 2003, pp. 981-985.

45. Edvardsen, C., "Water Permeability and Autogenous Healing of Cracks in Concrete," *ACI Materials Journal*, V. 96, No. 4, July-Aug. 1999, pp. 448-455.

46. Aldea, C.; Song, W.; Popovics, J. S.; and Shah, S. P., "Extent of Healing of Cracked Normal Strength Concrete," *Journal of Materials in Civil Engineering*, V. 12, 2000, pp. 92-96.

47. Clear, C. A., "The Effects of Autogenous Healing Upon the Leakage of Water through Cracks in Concrete," Cement and Concrete Association, Wexham Springs, 1985, p. 28.

48. Lepech, M. D., and Li, V. C., "Water Permeability of Cracked Cementitious Composites," ICF 11, Turin, Italy, Paper 4539 of Compendium of Papers, 2005. (CD-ROM)

49 Li, V. C.; Wang, S.; and Wu, C., "Tensile Strain-Hardening Behavior of Polyvinyl Alcohol Engineered Cementitious Composite (PVA-ECC)," *ACI Materials Journal*, V. 98, No. 6, Nov.-Dec. 2001, pp. 483-492.

50. Li, V. C.; Wu, C.; Wang, S.; Ogawa, A.; and Saito, T., "Interface Tailoring for Strain-Hardening PVA-ECC," *ACI Materials Journal*, V. 99, No. 5, Sept.-Oct. 2002, pp. 463-472.

51. Stang, H., "Scale Effects in FRC and HPRFCC Structural Elements," *High Performance Fiber Reinforced Cementitious Composites*, RILEM Proceedings Pro 30, A. E. Naaman and H. W. Reinhardt, eds., 2003, pp. 245-258.

52. Marshall, D. B., and Cox, B. N., "A J-Integral Method for Calculating Steady-State Matrix Cracking Stresses in Composites," *Mechanics of Materials*, V. 7, No. 2, 1988, pp. 127-133.

53. Li, V. C., and Leung, C. K. Y., "Theory of Steady State and Multiple Cracking of Random Discontinuous Fiber Reinforced Brittle Matrix Composites," *Journal of Engineering Mechanics*, ASCE, V. 118, No. 11, 1992, pp. 2246-2264.

54. Griffith, A. A., "The Phenomena of Rupture and Flow in Solids," *Philosophical Transactions of the Royal Society of London*, A 221, 1921, pp. 163-198, http://www.cmse.ed.ac.uk/AdvMat45/Griffith20.pdf.

55. ASTM E1304-97(2008)e1, "Standard Test Method for Plane-Strain Fracture Toughness of Metallic Materials," ASTM International, West Conshohocken, PA, 2008.

56. ASTM C511-02, "Standard Specification for Moist Cabinets, Moist Rooms, and Water Storage Tanks Used in the Testing of Hydraulic Cements and Concretes," ASTM International, West Conshohocken, PA.

57. Delagrave, A.; Pigeon, M.; Marchand, J.; and Revertegat, E., "Influence of Chloride Ions and pH Level on the Durability of High Performance Cement Pastes (Part II)," *Cement and Concrete Research*, V. 26, No. 5, May 1996, pp. 749-760.

58. Wang, K.; Nelsen, D. E.; and Nixon, W. A., "Damaging Effects of Deicing Chemicals on Concrete Materials," *Cement and Concrete Composites*, V. 28, No. 2, Feb. 2006, pp. 173-188.

59. Kabele, P.; Novak, L.; Nemecek, J.; and Pekar, J., "Multiscale Experimental Investigation of Deterioration of Fiber-Cementitious Composites in Aggressive Environment," *MHM 2007: Modelling of Heterogeneous Materials with Applications in Construction and Biomedcial Engineering*, June 2007, pp. 270-271.